[4] C. H. Grauling, Jr. and B. D. Geller, "A Broad-Band Frequency Translator with 30-dB Suppression of Spurious Sidebands," *IEEE Trans. Microwave Theory Tech.*, pp. 651–652, Sept. 1970.
[5] S. Rehnmark, "Theory and application of microwave couplers, phase shifters, and power dividers," Tech. Rep. 62, 1976, School of Electrical and Computer Engineering, Chalmers University of Technology, Gothenburg, Sweden.
[6] E. M. T. Jones and J. T. Bolljahn, "Coupled-strip-transmission-line filters and directional couplers," *IRE MTT*, pp. 75–81, Apr. 1956.
[7] D. M. Pozar, *Microwave Engineering*. Reading, MA: Addison-Wesley, 1990, pp. 415–430.
[8] G. B. Thomas, Jr., *Calculus and Analytic Geometry*. Reading, MA: Addison-Wesley, 1972, pp. 106–121.

A Microstrip Line on a Chiral Substrate

Michael S. Kluskens and Edward H. Newman

Abstract—**Right and left circular vector potentials are developed and used in a spectral-domain solution for a microstrip transmission line on a chiral substrate. These vector potentials have properties similar to those of the usual magnetic and electric vector potentials, except that they result in circular rather than linearly polarized fields, thereby simplifying field expansions in chiral media. The chiral microstrip line does not have bifurcated modes like other chiral guided wave structures; however, the chiral substrate causes a significant asymmetry in both the fields and currents.**

I. Introduction

This paper presents a spectral-domain Galerkin moment method (MM) solution for a microstrip transmission line on a chiral substrate. A chiral medium is a form of artificial dielectric consisting of chiral objects randomly embedded in a dielectric or other medium [1]. At optical frequencies, the chiral objects are molecules and the medium is called an isotropic optically active medium. At microwave frequencies, early research used conducting helices as a scale model for optical activity [2]. From this and later work, the constitutive relationships for chiral media have been shown to be the same as those for isotropic optically active media; therefore, the same notation is used [3, sec. 8.3].

A chiral medium is distinguished from other media in that right and left circularly polarized waves propagate through it with different phase velocities, even though it is a reciprocal and isotropic medium. For most chiral guided wave structures this property results in bifurcated modes [4]–[6], i.e., pairs of modes with the same cutoff frequency. The chiral microstrip line does not have bifurcated modes, and thus the dispersion curves are single valued. The primary effect of the chiral substrate is to generate asymmetric longitudinal and symmetric transverse fields. This effect could significantly alter the properties of microwave devices constructed on a chiral substrate.

Manuscript received March 1, 1991; revised July 8, 1991. This work was sponsored by the Joint Service Electronics Program under Contract N00014-78-C-0049 with the Ohio State University Research Foundation.

The authors are with the Department of Electrical Engineering, The Ohio State University, ElectroScience Laboratory, 1320 Kinnear Road, Columbus, OH 43212.

IEEE Log Number 9102813.

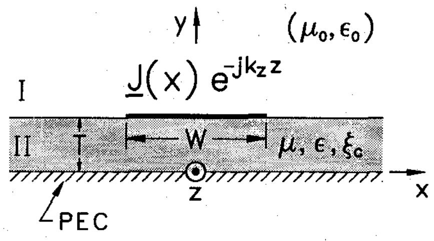

Fig. 1. Microstrip line on a grounded chiral substrate.

II. Theory

The constitutive relationships for a chiral medium can be written as

$$\boldsymbol{D} = \epsilon_c \boldsymbol{E} - j\mu\xi_c \boldsymbol{H} \tag{1}$$

$$\boldsymbol{B} = \mu \boldsymbol{H} + j\mu\xi_c \boldsymbol{E} \tag{2}$$

where $\epsilon_c = \epsilon + \mu\xi_c^2$, μ is the permeability, ϵ is the permittivity, and the pseudoscalar ξ_c is the chirality admittance of the medium ($e^{j\omega t}$).

Following the techniques used in [7], [8], the right ($\boldsymbol{R}$) and left ($\boldsymbol{L}$) circular vector potentials are defined as

$$\boldsymbol{R} = \hat{a}\psi(k_R) \tag{3}$$

$$\boldsymbol{L} = \hat{a}\psi(k_L) \tag{4}$$

where $\hat{a}$ is an arbitrary unit vector and $\psi(k)$ is a solution of the scalar wave equation $\nabla^2\psi(k) + k^2\psi(k) = 0$. The right and left circularly polarized electric fields are formed using

$$\boldsymbol{E}_R = \nabla \times \left(\boldsymbol{R} + \frac{1}{k_R} \nabla \times \boldsymbol{R} \right) \tag{5}$$

$$\boldsymbol{E}_L = \nabla \times \left(\boldsymbol{L} - \frac{1}{k_L} \nabla \times \boldsymbol{L} \right) \tag{6}$$

where the wave numbers k_R and k_L are given by

$$\left.\begin{matrix} k_R \\ k_L \end{matrix}\right\} = \omega\sqrt{\mu\epsilon_c} \pm \omega\mu\xi_c. \tag{7}$$

The corresponding magnetic fields are given by

$$\begin{pmatrix} \boldsymbol{H}_R \\ \boldsymbol{H}_L \end{pmatrix} = \frac{j}{\eta_c} \begin{pmatrix} \boldsymbol{E}_R \\ -\boldsymbol{E}_L \end{pmatrix} \tag{8}$$

where $\eta_c = \sqrt{\mu/\epsilon_c}$ is the chiral wave impedance. The right (or left) circular vector potential component R_y (or L_y) produces a right (or left) circular to y field RC_Y (or LC_Y), just as the magnetic vector potential component A_y produces a transverse magnetic to y field TM_Y.

The microstrip line is shown in Fig. 1, where the substrate has parameters (μ, ϵ, ξ_c) and thickness T. The microstrip line is W wide, infinitely thin, and perfectly conducting with a current distribution of $\boldsymbol{J}(x)e^{-jk_z z}$. The region $y > T$ is free space, with parameters (μ_0, ϵ_0) and wave number $k_0 = \omega\sqrt{\mu_0\epsilon_0}$. In this region the fields may be expanded as the sum of TM_Y field and a TE_Y field using

$$\begin{pmatrix} \boldsymbol{A} \\ \boldsymbol{F} \end{pmatrix} = \frac{\hat{y}}{2\pi} \int_{-\infty}^{\infty} \begin{pmatrix} \tilde{A} \\ \tilde{F} \end{pmatrix} e^{-j(k_x x + k_y y + k_z z)}\, dk_x \tag{9}$$

where $k_y^2 = k_x^2 + k_z^2 - k_0^2$.

In the substrate, the fields are expanded in terms of right and left circular vector potentials. Individually, right or left circularly polarized fields can not satisfy the boundary condition of zero tangential electric field on the ground plane at $y=T$. However, this boundary condition can be satisfied by a quasi-TM_Y field formed as the sum of a RC_Y field and a LC_Y field generated by the circular vector potentials [8]:

$$\begin{pmatrix} \boldsymbol{R}_{Y,M} \\ \boldsymbol{L}_{Y,M} \end{pmatrix} = \frac{\hat{y}}{2\pi}\int_{-\infty}^{\infty} \tilde{Q}_M \begin{pmatrix} \cos k_{y,R}y \\ -\cos k_{y,L}y \end{pmatrix} e^{-j(k_x x + k_z z)}\, dk_x \quad (10)$$

where $k_{y,R}^2 = k_x^2 + k_z^2 - k_R^2$ and $k_{y,L}^2 = k_x^2 + k_z^2 - k_L^2$. The resulting field is TM_Y if $\xi_c = 0$; hence the name quasi-TM_Y. Similarly, a quasi-TE_Y field can be formed using

$$\begin{pmatrix} \boldsymbol{R}_{Y,E} \\ \boldsymbol{L}_{Y,E} \end{pmatrix} = \frac{\hat{y}}{2\pi}\int_{-\infty}^{\infty} \tilde{Q}_E \begin{pmatrix} \dfrac{k_R}{k_{y,R}} \sin k_{y,R}y \\ \dfrac{k_L}{k_{y,L}} \sin k_{y,L}y \end{pmatrix} e^{-j(k_x x + k_z z)}\, dk_x. \quad (11)$$

The four unknown spectral functions $\tilde{A}$, $\tilde{F}$, $\tilde{Q}_M$, and $\tilde{Q}_E$ are determined by enforcing the boundary conditions at $y=T$ [8]. The fields E_x and E_z at the interface $y=T$ are presented below in terms of the even and odd components of the Fourier transforms of these fields generated by $\hat{x}$ and $\hat{z}$ polarized traveling wave line sources at $x=0$, $y=T$:

$$\tilde{E}_{x,e}^{J_x} = \frac{1}{\Delta}\left[\left(k_x^2 \frac{k_y}{\omega\mu_0} + k_z^2 \frac{\omega\epsilon_0}{k_y}\right)(1-S) - \frac{j}{\eta_c}\left(k_x^2 U + k_z^2 V\right)\right] \quad (12)$$

$$\tilde{E}_{z,e}^{J_z} = \frac{1}{\Delta}\left[\left(k_x^2 \frac{\omega\epsilon_0}{k_y} + k_z^2 \frac{k_y}{\omega\mu_0}\right)(1-S) - \frac{j}{\eta_c}\left(k_x^2 V + k_z^2 U\right)\right] \quad (13)$$

$$\tilde{E}_{z,o}^{J_x} = \tilde{E}_{x,o}^{J_z} = \frac{k_x k_z}{\Delta}\left[\left(\frac{k_y}{\omega\mu_0} - \frac{\omega\epsilon_0}{k_y}\right)(1-S) + \frac{j}{\eta_c}(V-U)\right] \quad (14)$$

$$\tilde{E}_{x,o}^{J_x} = -\tilde{E}_{z,o}^{J_z} = j\frac{2k_x k_z}{\eta_c \Delta} G^- \quad (15)$$

$$\tilde{E}_{z,e}^{J_x} = \tilde{E}_{x,e}^{J_z} = j\frac{k_z^2 - k_x^2}{\eta_c \Delta} G^- \quad (16)$$

where

$$\Delta = \left(k_x^2 + k_z^2\right)\left\{\left[\frac{\epsilon_c}{\mu}(1+S) - \frac{\epsilon_0}{\mu_0}(1-S)\right] + j\left[\frac{k_2}{k_y}\frac{\epsilon_0}{\mu}U + \frac{k_y}{k_2}\frac{\epsilon_c}{\mu_0}V\right]\right\} \quad (17)$$

$$G^{\pm} = \frac{1}{2}\left(\frac{k_R}{k_{y,R}}\frac{k_{y,L}}{k_L} \pm \frac{k_{y,R}}{k_R}\frac{k_L}{k_{y,L}}\right)\sin k_{y,R}T \sin k_{y,L}T \quad (18)$$

$$S = \cos k_{y,R}T \cos k_{y,L}T - G^+ \quad (19)$$

$$U = \frac{k_{y,R}}{k_R}\sin k_{y,R}T \cos k_{y,L}T + \frac{k_{y,L}}{k_L}\sin k_{y,L}T \cos k_{y,R}T \quad (20)$$

$$V = \frac{k_R}{k_{y,R}}\sin k_{y,R}T \cos k_{y,L}T + \frac{k_L}{k_{y,L}}\sin k_{y,L}T \cos k_{y,R}T \quad (21)$$

with $k_2 = \omega\sqrt{\mu\epsilon_c} = (k_R + k_L)/2$. For example, the E_x field generated by the surface current $J_z(x)$ is given by

$$E_x^{J_z}(x) = \frac{1}{2\pi}\int_{-\infty}^{\infty}\left[\tilde{E}_{x,e}^{J_z}(k_x) + \tilde{E}_{x,o}^{J_z}(k_x)\right] \cdot \tilde{J}_z(k_x) e^{-j(k_x x + k_z z)}\, dk_x. \quad (22)$$

In a conventional achiral microstrip line $\tilde{E}_{x,o}^{J_x}$, $\tilde{E}_{z,o}^{J_z}$, $\tilde{E}_{z,e}^{J_x}$, and $\tilde{E}_{x,e}^{J_z}$ are zero, causing $J_z(x)$ and $J_x(x)$ to be even and odd functions of x, respectively. However, this is not true for a chiral microstrip line, thereby requiring a set of even and odd basis functions.

III. Moment Method Solution

The J_x and J_z currents for the MM solution are expanded as

$$J_x(x) = \sum_{n=0}^{N_x} I_{x,n} J_{x,n}(x) \quad (23)$$

$$J_z(x) = \sum_{n=0}^{N_z} I_{z,n} J_{z,n}(x) \quad (24)$$

where $I_{x,n}$ and $I_{z,n}$ are the unknown coefficients. The basis functions $J_{x,n}$ and $J_{z,n}$ are Chebyshev polynomials weighted by the edge conditions [9]–[13]:

$$J_{x,n}(x) = \frac{4}{\pi W}\frac{U_n(2x/W)}{n+1}\sqrt{1-(2x/W)^2} \quad (25)$$

$$J_{z,n}(x) = \frac{2}{\pi W} T_n(2x/W) \Big/ \sqrt{1-(2x/W)^2} \quad (26)$$

where $T_n(x)$ and $U_n(x)$ are Chebyshev polynomials of the first and second kinds, respectively. The Fourier transforms of these basis functions are [14, sec. 6.671]:

$$\tilde{J}_{x,n}(k_x) = 2j^n \frac{J_{n+1}(k_x W/2)}{k_x W/2} \quad (27)$$

$$\tilde{J}_{z,n}(k_x) = j^n J_n(k_x W/2) \quad (28)$$

where $J_n(x)$ is an nth-order Bessel function. The MM can then be applied to enforce the boundary condition of zero tangential electric field on the microstrip line. In block matrix form, the MM equation is

$$\begin{bmatrix} Z_{xx} & Z_{xz} \\ Z_{zx} & Z_{zz} \end{bmatrix}\begin{bmatrix} I_x \\ I_z \end{bmatrix} = \begin{bmatrix} 0 \\ 0 \end{bmatrix} \quad (29)$$

where $I_x = [I_{x,0} \cdots I_{x,N_x}]^T$ and $I_z = [I_{z,0} \cdots I_{z,N_z}]^T$.

In the xz block

$$Z_{xz} = \begin{bmatrix} Z_{xz(0,0)} & \cdots & Z_{xz(0,N_z)} \\ \vdots & \ddots & \vdots \\ Z_{xz(N_x,0)} & \cdots & Z_{xz(N_x,N_z)} \end{bmatrix} \quad (30)$$

$$Z_{xz(m,n)} = -\int_{-\infty}^{\infty} \tilde{E}_x^{J_z}(k_x)\tilde{J}_{z,n}(k_x)\tilde{J}_{x,m}(-k_x)\, dk_x. \quad (31)$$

Impedance elements in the remaining blocks are given similarly.

The propagation constants of the modes are found as the roots of the determinant of the impedance matrix given in (29). For a given propagation constant the fields in any region and the current distribution may be found using the equations presented in the previous section.

IV. Numerical Results

This section presents numerical results demonstrating the accuracy of the MM solution, and some effects of chirality on a microstrip transmission line. All currents are normalized to

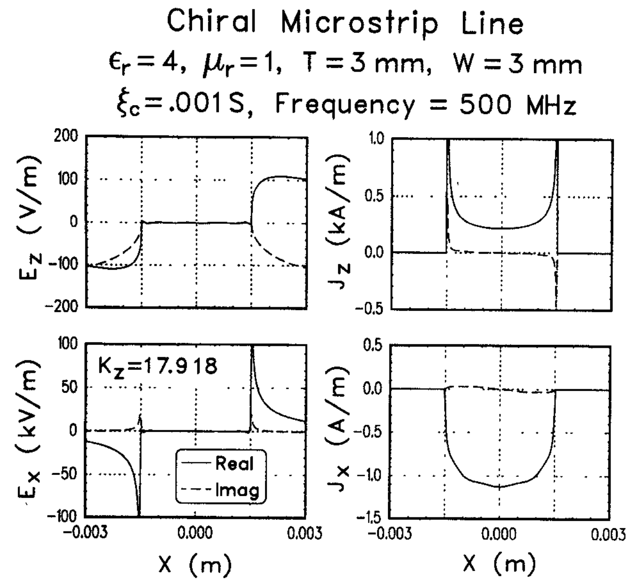

Fig. 2. Fields and currents at $y = T$ for a chiral microstrip solved using ten J_z modes and ten J_x modes.

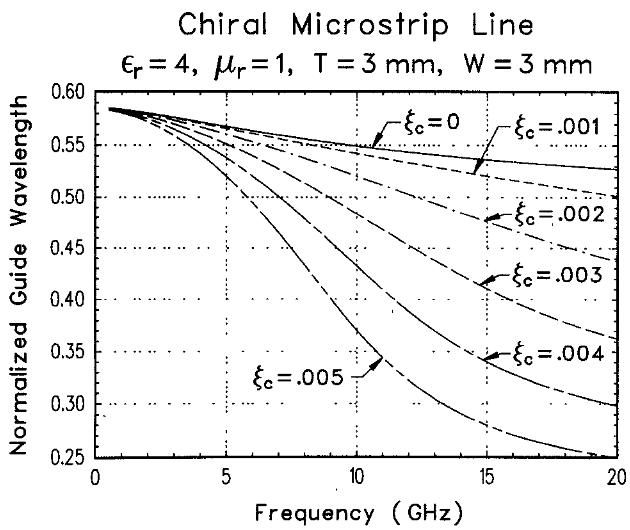

Fig. 3. Normalized guide wavelength (λ_g / λ_0) versus frequency for the fundamental mode of chiral and achiral microstrip lines, for a range of chiral parameters in Siemens.

$I_{z,0} = 1$, since the microstrip current can only be found to within a constant. In the figures the real part of the current and fields is shown as a solid line, and the imaginary part as a dashed line.

Fig. 2 shows the electric fields and currents at the interface $y = T$ for a MM solution using ten longitudinal and ten transverse basis functions. The left-hand graphs show that the fields satisfy the boundary condition of zero tangential electric field on the microstrip line. The corresponding currents are shown in the right-hand graphs. The even transverse current component, which occurs solely because of the chirality, is significantly larger than the odd transverse current component.

The dispersion curve shown in Fig. 3 shows the normalized guide wavelength (λ_g / λ_0) for the fundamental mode of a chiral microstrip line, for a range of chiral parameters. The case $\xi_c = 0$ corresponds to an achiral line. Fig. 3 shows that the propagation constant is not significantly affected unless the chiral parameter is a significant percentage of the maximum value set in [15] of $\xi_{c,\max} = \sqrt{\epsilon / \mu}$, which in this case is 0.0053 S.

References

[1] D. L. Jaggard, A. R. Mickelson, and C. H. Papas, "On electromagnetic waves in chiral media," *Appl. Phys.*, vol. 18, pp. 211–216, 1979.

[2] I. Tinoco, Jr. and M. P. Freeman, "The optical activity of oriented copper helices. I. Experimental," *J. Phys. Chem.*, vol. 61, pp. 1196–1200, Sept. 1957.

[3] E. J. Post, *Formal Structure of Electromagnetics*. Amsterdam: North-Holland, 1962.

[4] C. Eftimiu and L. W. Pearson, "Guided electromagnetic waves in chiral media," *Radio Science*, vol. 24, pp. 351–359, May/June 1989.

[5] P. Pelet and N. Engheta, "The theory of chirowaveguides," *IEEE Trans. Antennas Propagat.*, vol. AP-38, pp. 90–98, Jan. 1990.

[6] J. A. M. Svedin, "Propagation analysis of chirowaveguides using the finite-element method," *IEEE Trans. Microwave Theory Tech.*, vol. 38, pp. 1488–1496, Oct. 1990.

[7] M. S. Kluskens and E. H. Newman, "Scattering by a multilayer chiral cylinder," *IEEE Trans. Antennas Propagat.*, vol. AP-39, pp. 91–96, Jan. 1991.

[8] M. S. Kluskens, "Method of moments analysis of scattering by chiral media," Ph.D. dissertation, The Ohio State University, Columbus, June 1991.

[9] R. E. Collin, *Field Theory of Guided Waves*. New York: IEEE Press, 1991.

[10] T. Kitazawa and Y. Hayashi, "Propagation characteristics of striplines with multilayered anisotropic media," *IEEE Trans. Microwave Theory Tech.*, vol. 31, pp. 429–433, June 1983.

[11] F. Medina, M. Horno, and H. Baudrand, "Generalized spectral analysis of planar lines on layered media including uniaxial and biaxial dielectric substrates," *IEEE Trans. Microwave Theory Tech.*, vol. 37, pp. 504–511, Mar. 1989.

[12] M. Kobayashi and T. Iijima, "Frequency-dependent characteristics of current distributions on microstrip," *IEEE Trans. Microwave Theory Tech.*, vol. 37, pp. 799–801, Apr. 1989.

[13] Y. Yuan and D. P. Nyquist, "Full-wave perturbation theory based upon electric field integral equations for coupled microstrip transmission lines," *IEEE Trans. Microwave Theory Tech.*, vol. 38, pp. 1576–1584, Nov. 1990.

[14] I. S. Gradshteyn and I. M. Ryzhik, *Table of Integrals, Series, and Products*. Orlando, FL: Academic, 1980.

[15] N. Engheta and D. L. Jaggard, "Electromagnetic chirality and its applications," *IEEE Antennas and Propagation Society Newsletter*, vol. 30, pp. 6–12, Oct. 1988.

Time-Domain Scattering Parameters of an Exponential Transmission Line

Ching-Wen Hsue

Abstract —**The scattering parameters of an exponential line are studied in detail both in frequency and time domains. By taking the causality condition into consideration, we cast the time domain scattering parameters in a rapid-convergence power series. Each term of the power series represents a signal component generated by the exponential line when the signal travels a round trip.**

Manuscript received April 30, 1991; revised June 17, 1991.

The author is with AT&T Bell Laboratories, P.O. Box 900, Princeton, NJ 08540.

IEEE Log Number 9102815.

0018-9480/91$01.00